Transport and Communications Science Journal

DEEP LEARNING ARCHITECTURE TO PREDICT NATURAL VIBRATION FREQUENCIES OF DAMAGED STRUCTURES

Thanh Sang To*, Hieu Nguyen-Van

University of Architecture Ho Chi Minh City, Ho Chi Minh City, Vietnam

ARTICLE INFO

TYPE: Research Article
Received: 04/03/2026
Revised: 04/06/2026
Accepted: 03/07/2026
Published online: 15/09/2026
https://doi.org/10.47869/tcsj.77.7.5
* *Corresponding author*
Email: sang.tothanh@uah.edu.vn;

Abstract. Structural damage can arise from various unforeseen causes. Such damage exerts a substantial impact on the load-carrying capacity of the structure. In this study, we propose a Deep Neural Network (DNN) serving as a surrogate model to determine the severity of damage in beam structures Initially, a finite element model (FEM) was constructed in MATLAB to generate the training and testing datasets. Subsequently, a multi-layer deep learning architecture utilizing an artificial neural network is constructed. The Deep Neural Network is trained on this dataset, which encompasses numerous damage scenarios, to predict the output parameters (specifically, the first three natural frequencies of the structure). The reliability of the Deep Neural Network was subsequently verified on the test dataset, achieving an R^2value greater than 0.99. Consequently, this Deep Neural Network can serve as a substitute for the finite element method, thereby significantly accelerating the model updating process within the damage prediction framework.

Keywords: DNN, Natural Frequency, Surrogate Model, Structural Health Monitoring, SHM.

1. INTRODUCTION

Structures can suffer damage from various causes during their service life, such as the impact of wind loads, earthquakes, or corrosive environments. Therefore, assessing the severity of structural damage by determining the changes in their natural frequencies holds significant academic and practical value. In recent years, the field of Structural Health Monitoring (SHM) has attracted immense interest from scholars worldwide [1-3].

Along with the rapid development of modern computational methods such as intelligent algorithms [4-7], Artificial Intelligence (AI) models [8-10] have provided powerful tools to further advance the field of structural health monitoring [11-13].

To advance the automation of structural diagnostics, Hasani al et. developed a novel AI-driven methodology [14]. By coupling frequency-spatial analysis with stochastic subspace identification, the system can autonomously extract modal parameters. This is complemented by a hybrid anomaly detector based on a conditional variational autoencoder (SSA-OC-SVM). Empirical evaluations demonstrated the model's proficiency in accurately classifying failure events across nine separate structural locations, highlighting its superior reliability, computational scalability, and accuracy as a promising paradigm for next-generation intelligent SHM.

Addressing the complex challenge of multi-damage identification, Guilherme Ferreira Gomes and Vinicius Dammenhain Takano [15] present a hybrid approach leveraging the Sunflower Optimization (SFO) algorithm alongside Machine Learning (ML) and Artificial Neural Network (ANN) models. Delaminations were simulated as elliptical defects within a square composite laminate using finite element analysis. Strain data from forward modelling validated the SFO's robust convergence in detecting one or two damages.

Additionally, a newly generated strain dataset enabled the rigorous training of AI models for damage classification and parameter regression. Results demonstrated near 100% accuracy in classifying the damage quantity. In isolated damage scenarios, the regression models achieved 99% accuracy for defect positioning and 49% for sizing. Nonetheless, parameter estimation for multiple defects-notably three damages for SFO and multiple damages for ML models-yielded diminished accuracy, highlighting the severe computational intricacies of multi-delamination scenarios.

Existing studies substantiate the effectiveness of advanced artificial intelligence approaches in structural damage prognosis, underscoring the substantial attention and resources directed toward this critical issue by the international scientific community. The present research is dedicated to utilizing a Deep Neural Network (DNN) to forecast the vibration frequencies of compromised structures, thereby establishing an AI-driven predictive model to facilitate computational model updating in subsequent damage diagnosis applications.

This manuscript is structured into six sections, commencing with the Introduction detailed above. Section 2 (Methodology) elucidates the theoretical foundations, analytical tools, and the procedural framework of the proposed methodology. Section 3 (Building Finite Element Model and Collecting Data) delineates the construction of the FEM model, which serves to generate the requisite training data. Section 4 (Deep Neural Network) explicates the architectural design and formulation of the DNN. Section 5 (Results and Discussion) provides a comprehensive presentation and discussion of the analytical results. Ultimately, Section 6 (Conclusion) encapsulates the primary conclusions derived from this investigation

2. METHODOLOGY

This study is predicated on the integration of the FEM and DNN. Within this framework, FEM is utilized to generate the training datasets, whereas the DNN is trained to establish a surrogate model. This surrogate model can subsequently be employed for future model updating in iterative tasks associated with SHM problems, which would otherwise incur prohibitive computational costs if relying exclusively on conventional FEM. The specific architecture of this proposed methodology is illustrated in Figure 1 below.

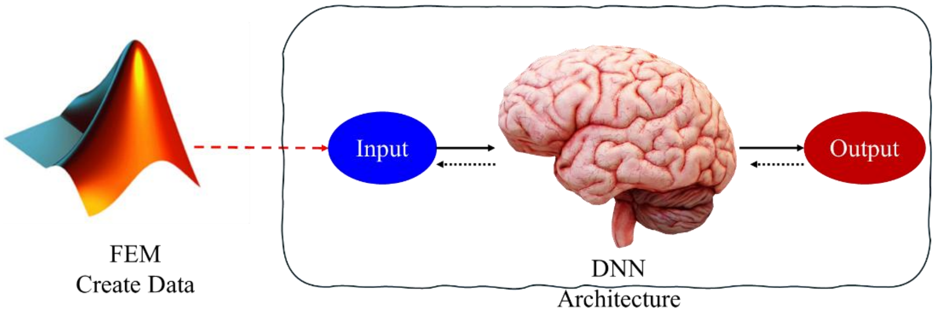

Figure 1. Proposal framework.

Initially, a baseline FEM of the beam is constructed in MATLAB to function as the data generation engine. This dataset is used to train the DNN via a dedicated architecture fine-tuned to the specific constraints of the problem. The input vector consists of the structural damage severity and location. To enhance the model's generalization ability, training scenarios are comprehensively expanded across a wide array of damage configurations. Ultimately, the DNN predicts the natural frequencies as output parameters, which can be readily adopted for subsequent damage diagnosis, effectively obviating the need for repetitive and time-consuming FEM computations.

3. BUILDING FINITE ELEMENT MODEL AND COLLECTING DATA

To generate training data and evaluate the performance of the DNN, a finite element model of the beam structure was established. In this study, Timoshenko beams are utilized to investigate the variations in free vibration frequencies under various damage scenarios [16]. As formulated in Eq. (1), the total kinetic energy consists of two parts: one associated with translation and the other with rotation.

$$T = \frac{1}{2}\int_{-a}^{a} \rho A\, \dot{w}^2 dx + \frac{1}{2}\int_{-a}^{a} \rho I_z \dot{\theta}^2\, dx \tag{1}$$

For the two-node element, the corresponding stiffness and mass matrices are established in Eqs. (2) and (3).

$$K^e = \int_{-1}^{1} \frac{EI_z}{a^2}\left(\frac{dN}{d\xi}\right)^T \left(\frac{dN}{d\xi}\right) ad\xi + \int_{-1}^{1} kGA\left(\frac{1}{a}\frac{dN}{d\xi}+N\right)^T \left(\frac{1}{a}\frac{dN}{d\xi}+N\right) ad\xi \tag{2}$$

$$M^e = \int_{-1}^{1} \rho A\, N^T N a d\xi + \int_{-1}^{1} \rho I_z N^T N a d\xi \tag{3}$$

To validate the model, a thin ($L = 1$, $h = 0.001$) cantilever beam is considered as the first problem, where the nondimensional natural frequencies are defined by Eq. (4).

$$\bar{\omega} = \omega L^2 \sqrt{\frac{\rho A}{EI_z}} \tag{4}$$

Given the dimensionless material properties, specifically the modulus of elasticity ($E = 10^7$) and Poisson's ratio ($\nu = 0.30$), the first five natural frequencies of the structure in its undamaged state are presented in Table 1, while the corresponding mode shapes are depicted in Figure 2. In this model, the FEM of the beam is meshed to 40.

Table 1. Non-dimensional natural frequencies for cantilever isotropic thin beam.

Natural frequencies	Mode 1	Mode 2	Mode 3	Mode 4	Mode 5
Value	3.5162	22.0682	61.9689	121.9783	202.8568

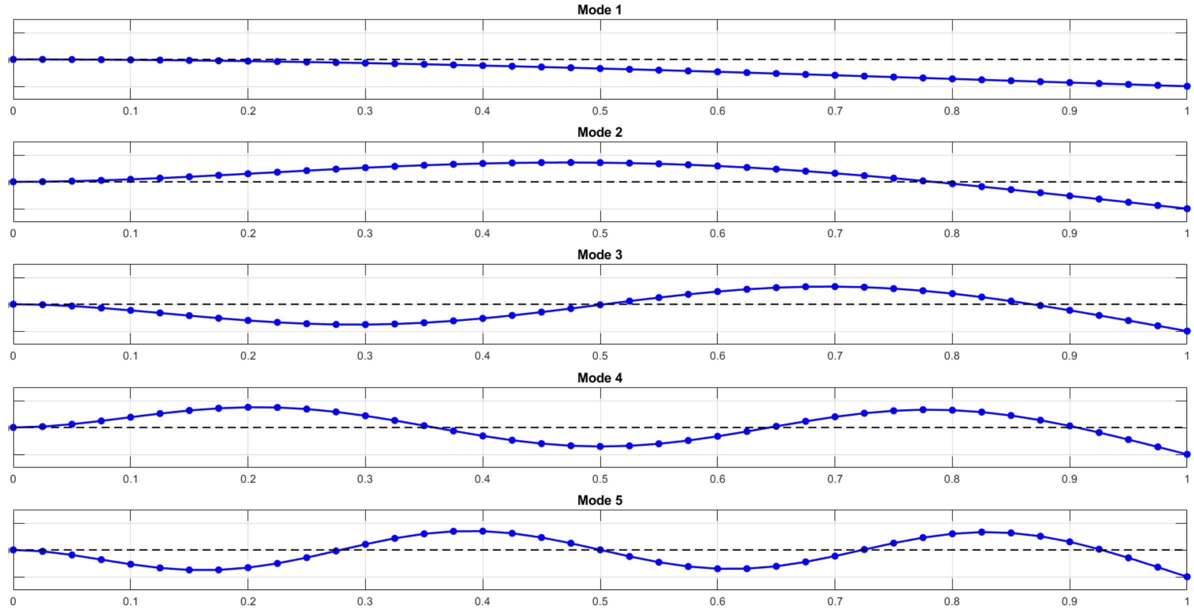

Figure 2. Mode shapes.

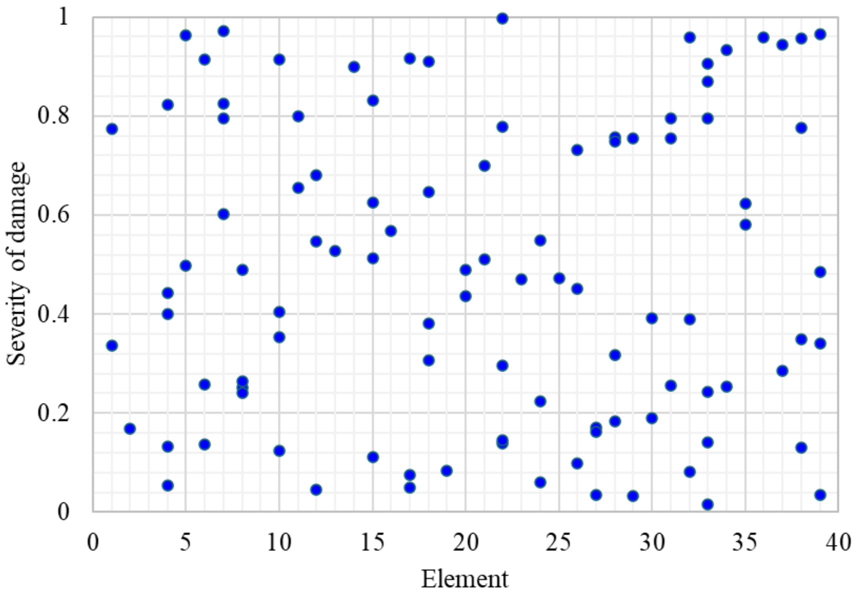

Figure 3. Damaged scenarios.

Subsequently, a comprehensive dataset was generated by randomly assigning the locations and severities of structural damage (see Figure 3). The FEM was then employed to compute the natural frequencies and corresponding mode shapes for these scenarios, as detailed in Table 2. Finally, the acquired dataset was partitioned into two subsets: 80% allocated for training the DNN model, and the remaining 20% reserved for evaluating its predictive accuracy.

Table 2. The natural frequencies of the beam corresponding to the damage scenarios.

No	$\overline{\omega_1}$	$\overline{\omega_2}$	$\overline{\omega_3}$	No	$\overline{\omega_1}$	$\overline{\omega_2}$	$\overline{\omega_3}$	No	$\overline{\omega_1}$	$\overline{\omega_2}$	$\overline{\omega_3}$	No	$\overline{\omega_1}$	$\overline{\omega_2}$	$\overline{\omega_3}$
1	3.516	22.060	61.866	**26**	3.486	22.030	61.372	**51**	3.489	22.053	61.940	**76**	2.987	17.818	57.296
2	3.505	22.056	61.969	**27**	3.490	20.253	56.156	**52**	3.466	21.946	60.844	**77**	3.516	22.068	61.963
3	3.457	18.791	54.850	**28**	3.397	21.847	61.913	**53**	3.448	22.029	61.896	**78**	3.494	21.521	61.961
4	3.464	22.002	60.943	**29**	3.516	22.068	61.958	**54**	3.479	22.049	61.375	**79**	3.511	22.045	61.830
5	3.516	22.068	61.969	**30**	3.481	20.434	60.031	**55**	3.515	21.956	61.399	**80**	3.199	20.382	56.580
6	3.513	22.066	61.965	**31**	3.512	21.585	57.942	**56**	3.261	18.348	61.229	**81**	3.515	21.879	60.032
7	3.516	22.068	61.963	**32**	3.508	21.828	61.959	**57**	3.508	22.067	61.882	**82**	3.404	22.057	60.710
8	3.514	21.568	56.399	**33**	3.516	22.068	61.959	**58**	3.494	22.055	61.945	**83**	2.860	20.597	60.791
9	3.513	22.030	61.918	**34**	3.423	19.295	61.244	**59**	3.516	22.066	61.968	**84**	3.516	22.068	61.967
10	3.516	22.063	61.915	**35**	3.224	21.749	61.960	**60**	3.357	21.650	61.616	**85**	3.360	16.833	56.794
11	3.384	15.663	48.553	**36**	3.516	21.915	59.920	**61**	3.511	22.059	61.967	**86**	3.378	22.055	60.434
12	3.516	22.065	61.920	**37**	3.514	21.812	58.989	**62**	3.468	21.796	61.276	**87**	3.480	17.246	37.840
13	3.515	21.962	61.427	**38**	3.517	22.065	61.906	**63**	3.516	22.056	61.820	**88**	2.925	19.870	58.048
14	3.514	21.732	59.519	**39**	3.259	22.024	61.075	**64**	3.328	21.580	61.559	**89**	3.514	21.906	61.495
15	3.491	20.350	56.407	**40**	3.508	21.537	60.921	**65**	3.499	22.059	61.684	**90**	3.508	21.541	60.489
16	3.432	16.245	44.666	**41**	3.507	22.012	61.751	**66**	3.513	22.022	61.939	**91**	3.480	20.843	61.640
17	2.646	21.101	50.944	**42**	3.508	21.645	61.433	**67**	3.273	22.027	61.126	**92**	3.508	21.154	55.995
18	3.488	21.989	61.901	**43**	3.516	22.053	61.700	**68**	2.953	21.489	61.953	**93**	3.500	20.681	56.138
19	3.508	21.371	58.734	**44**	3.515	22.014	61.475	**69**	3.516	22.047	61.648	**94**	3.489	21.905	61.348
20	3.517	22.060	61.805	**45**	3.486	21.811	61.365	**70**	3.428	19.406	61.272	**95**	3.506	20.719	51.036
21	3.468	21.357	61.522	**46**	2.286	19.728	60.167	**71**	3.516	22.050	61.700	**96**	3.516	22.068	61.959
22	3.516	22.025	61.579	**47**	3.512	21.908	61.925	**72**	3.474	21.813	61.008	**97**	3.488	21.397	61.959
23	3.419	22.051	61.629	**48**	3.516	22.056	61.740	**73**	3.153	18.812	58.217	**98**	3.450	21.101	61.365
24	3.500	21.816	61.809	**49**	3.502	21.465	61.558	**74**	3.056	22.024	57.252	**99**	3.499	21.547	61.947
25	3.516	21.979	61.403	**50**	3.222	20.587	58.519	**75**	3.244	22.022	61.027	**100**	3.516	22.047	61.714

4. DEEP NEURAL NETWORK

A Deep Neural Network is a biologically inspired computational framework designed to emulate the cognitive mechanisms of the human brain. Characterized by an intricate architecture comprising multiple layers and interconnected neurons, the DNN is highly adept at modeling complex information processing-a capability that defines the paradigm of 'deep learning' (see Figure 4). Operationally, the DNN relies on two fundamental processes: forward propagation and backpropagation. These iterative mechanisms facilitate the computation and optimization of internal parameters, enabling the model to implicitly learn predictive patterns from the input datasets. As a corollary, the predictive accuracy and overall robustness of the DNN are profoundly contingent upon the quality and representativeness of its training data.

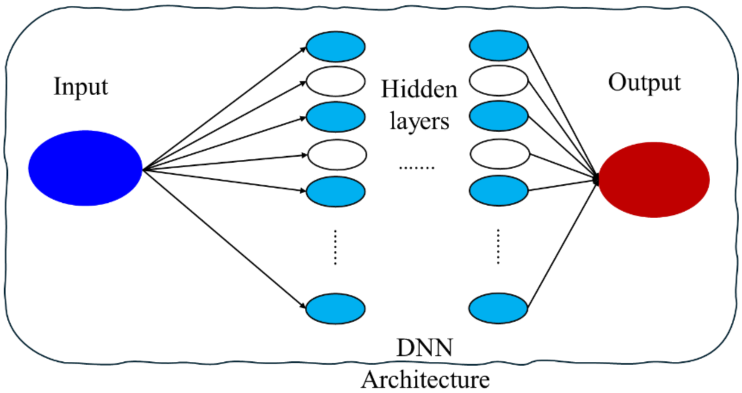

Figure 4. DNN Architecture.

At the core of this network's computational capacity is the activation function. Upon receiving input stimuli, an individual neuron computes a weighted sum, mathematically expressed as $Z = WX + b$. This aggregated value is subsequently processed by an activation function, which dictates both the activation threshold (i.e., whether the neuron 'fires') and the magnitude of the propagated signal. Crucially, the activation function serves to map non-linearities into the DNN, enabling it to solve complex, high-dimensional problems. While the literature presents a diverse array of activation functions-including ReLU, Tanh, and Softsign, etc.-the ReLU and Sigmoid functions (see Eqs. (5)-(6)) remain distinguished for their computational efficiency and ubiquitous empirical validation [17]. Accordingly, this study adopts the Sigmoid function as the primary activation element for the proposed DNN topology. Additionally, a deep network configuration comprising two hidden layers, with each layer containing sixteen neurons, is utilized in conjunction with the Adam optimization algorithm to construct the DNN in this study. Specifically, the input layer consists of two neurons representing the damage locations and corresponding severities at arbitrary positions along the beam, while the output layer yields the first three natural frequencies of the structure.

$$f(x) = \max(0, x) \tag{5}$$

$$f(x) = \frac{1}{1 + e^{-x}} \tag{6}$$

In order to evaluate the efficacy of the proposed model, statistical metrics including R^2, RMSE, and MAE are utilized. The exact formulations of these metrics are provided in Eqs. (7) to (9).

$$R^2 = 1 - \frac{\sum(y_i - \hat{y})^2}{\sum(y_i - \bar{y})^2} \tag{7}$$

$$RMSE = \sqrt{\frac{1}{n}\sum_{i=1}^{n}\left(Y_i - \hat{Y}_i\right)^2} \tag{8}$$

$$MAE = \frac{1}{n}\sum_{i=1}^{n}\left|Y_i - \widehat{Y_i}\right| \tag{9}$$

2. RESULTS AND DISCUSSION

Using damage severity and damage location as input parameters, the trained DNN yielded the results presented in Table 3. The evaluation metrics indicate that the deep learning model achieved highly impressive performance, with an R^2 value of 0.99962. This near-perfect score demonstrates the robust predictive capability of the DNN. Furthermore, the error metrics are remarkably low, at RMSE = 0.65953 and MAE = 0.26249, respectively. These findings confirm that the predictions generated by the DNN are in excellent agreement with the actual results derived from the FEM.

Table 3. Results obtained from the training process of DNN.

Measurement	R^2	RMSE	MAE
Value	0.99962	0.65953	0.26249

The training progression of the DNN on the primary dataset is presented in Figure 5. It is observed that the training performance undergoes significant improvement following roughly 150,000 epochs. The predictive capability subsequently experiences continuous enhancement up to epoch 751,000, reaching a terminal value of 0.00212029.

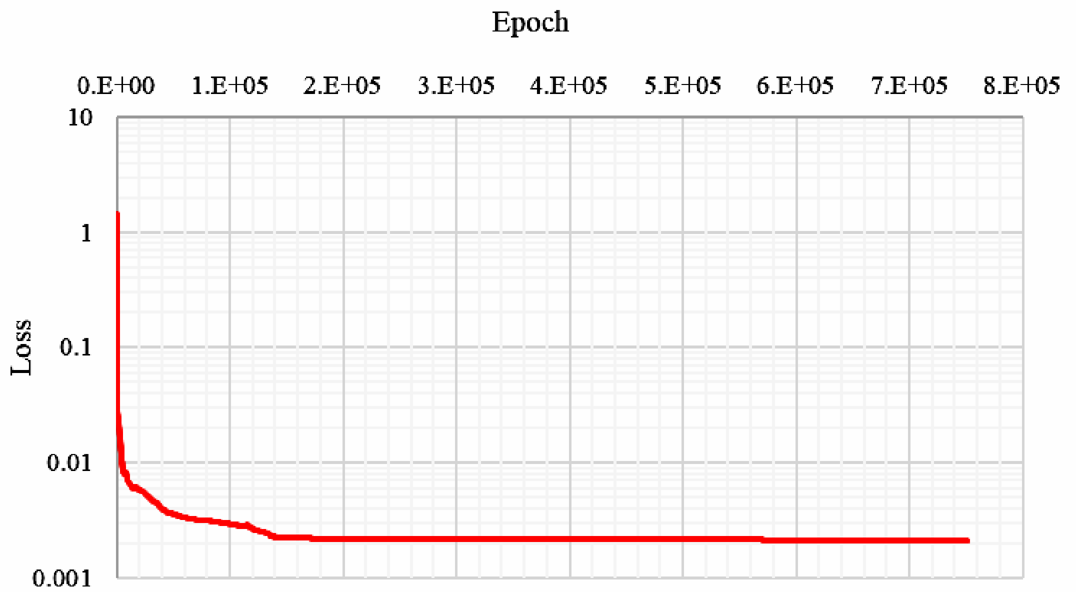

Figure 5. Loss function during training process.

Figure 6 to Figure 8 illustrate the prediction results of the first three natural frequencies of the beam using the DNN model compared to the values obtained from the FEM. As previously stated, 80% of the dataset was utilized for training, while the remaining 20% was reserved for testing. The blue markers represent the outcomes from the training phase, whereas the green markers denote the independent testing results of the DNN on unseen data.

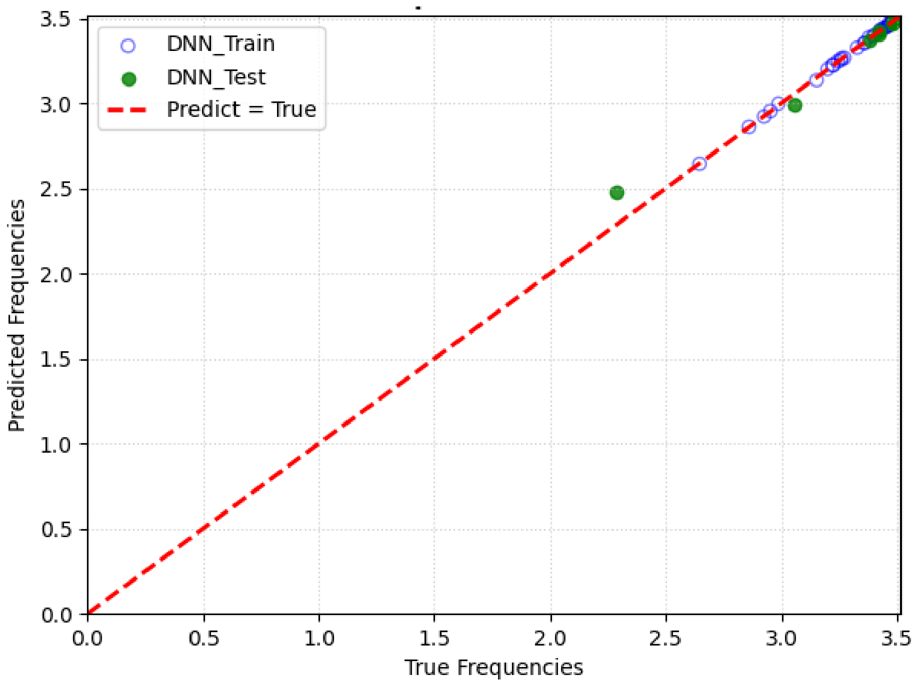

Figure 6. DNN Train and Test for the first natural frequency of beam.

Figure 6 presents the obtained results for the first mode. Given the high accuracy with an R^2 value of 0.99962 reported in Table 3, it is evident that the natural frequency of mode 1 is estimated with remarkable precision using the DNN model compared to conventional FEM. Furthermore, the robustness of the DNN model ensures that the independent testing values are also predicted reliably. Although there is a single outlier exhibiting a discrepancy of approximately 8% between the DNN prediction and the FEM value, this deviation remains within an acceptable range.

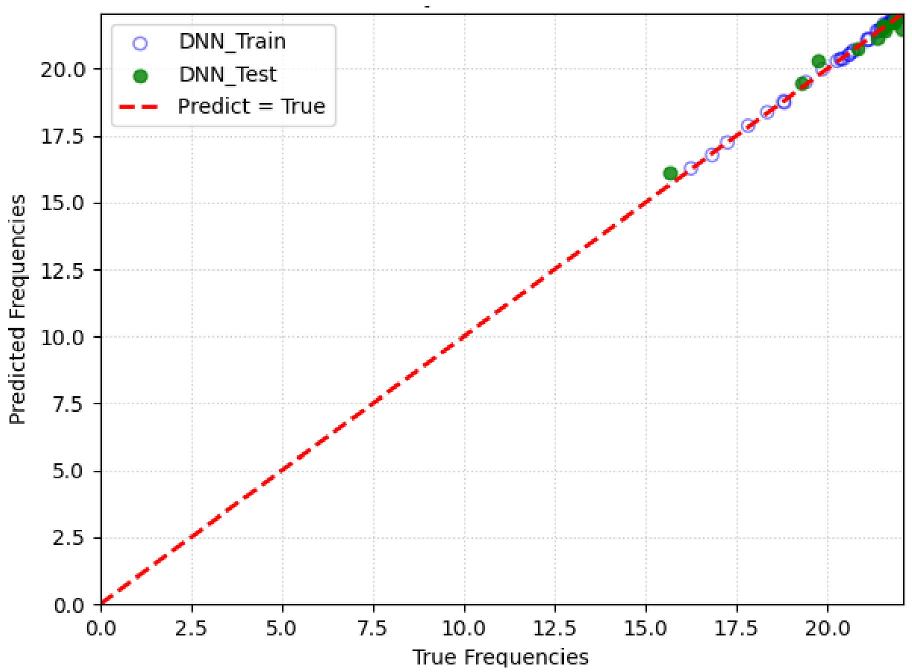

Figure 7. DNN Train and Test for the second natural frequency of beam.

In comparison to the first mode, the natural frequency of the second mode is predicted with remarkable precision across both the training and testing datasets, with detailed results illustrated in Figure 7. Notably, the red reference line-representing the perfect correlation between the DNN computations and FEM simulations-intersects nearly all scatter points. This strong alignment confirms that the DNN-estimated values are highly compatible with the finite element model, thereby validating the network's efficacy in approximating the second-mode natural frequency.

Figure 8 depicts the third vibration mode of the beam. Consistent with the preceding modes, the results underscore the DNN's viability as a robust surrogate for the FEM in predicting this third-mode frequency. The red dashed line is again shown to traverse the vast majority of the data points in both sets, substantiating the overall effectiveness of the methodology. An isolated outlier lies outside this trajectory, exhibiting an estimation error of roughly 8%; however, analogous to the observation in the first mode, this minor deviation remains within an acceptable tolerance.

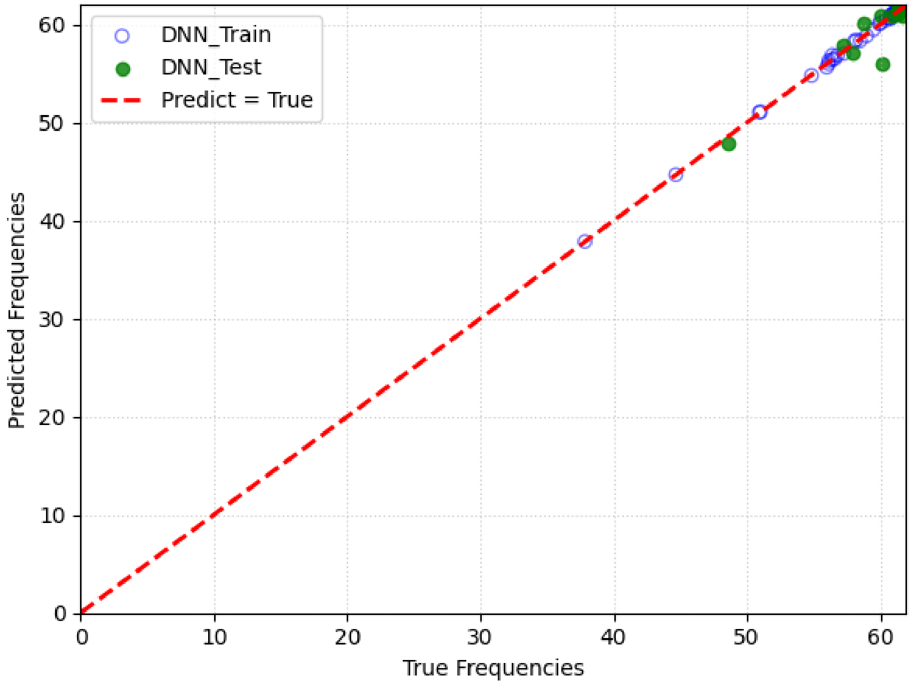

Figure 8. DNN Train and Test for the third natural frequency of beam.

6. CONCLUSION

This study introduces an advanced artificial intelligence methodology for forecasting the natural frequencies of compromised structures, establishing a fundamental basis for the identification of damage severity and localization. Derived from the findings presented in this paper, the primary conclusions are summarized as follows:

1) A multi-layer deep learning framework, conceptualized on the computational architecture of the human brain, was proposed and successfully implemented for the natural frequency prediction of damaged structures.
2) Leveraging the robust performance of the DNN, the structural vibration frequencies across diverse scenarios of damage location and severity were accurately estimated.

3) The precision of the proposed model is substantiated by the quantitative evaluation metrics, notably an R^2 value converging to unity, coupled with an RMSE of 0.65953 and a MAE of 0.26249

ACKNOWLEDGMENT

This research received funding by University of Architecture Ho Chi Minh City under grant number NCKH25-XD02

REFERENCES

[1]. T. Sang-To, S. Khatir, H. Le-Minh and T. Cuong-Le, Damage detection of steel roof systems using planet optimization algorithm, Journal of Soft Computing in Civil Engineering, 9 (2025) 78-94. https://doi.org/10.22115/scce.2024.452343.1844

[2]. H. Minh, T. Sang-To, B. Le-Van and T. Cuong-Le, Optimization of high-rise concrete structure using a sequence design based on a proposed surrogate model (PSM) and finite element (FE) model updating, Archives of Civil and Mechanical Engineering, 25 (2025) 243. https://doi.org/10.1007/s43452-025-01296-2

[3]. N. Tran, H. Nguyen, T. Nguyen, T. Bui and L. Wang, An advanced hybrid deep learning framework for structural health monitoring of cable-stayed bridge model using fiber optic sensors, Structures, 82 (2025) 110596. https://doi.org/10.1016/j.istruc.2025.110596

[4]. T. S. To, Q. Thien-Huynh, L. Bui and T. Cuong-Le, A Calibrated Framework Integrating Three-Dimensional Numerical Modeling with an Optimization Algorithm for the Estimation of Soil–Pile Interaction,Transportation Infrastructure Geotechnology, 13 (2026) 36. https://doi.org/10.1007/s40515-025-00783-6

[5]. T. Sang-To, T. Tran and T. Cuong-Le, Investigation of the Effectiveness of Optimization Algorithms in Structures, 747 (2025) 241-248. https://doi.org/10.1007/978-3-032-04645-1_29

[6]. L. YiFei, C. MaoSen, T. N. Hoa, S. Khatir, H.-L. Minh, T. SangTo, T. Cuong-Le and M. A. Wahab, Metamodel-assisted hybrid optimization strategy for model updating using vibration response data, Advances in Engineering Software, 185 (2023) 103515. https://doi.org/10.1016/j.advengsoft.2023.103515

[7]. T. To, H. Minh, T. Huynh, S. Khatir, M. Wahab and T. Cuong-Le, A nonlinear optimization method for calibration of large-scale deep cement mixing in very soft clay deep excavation, International Journal for Numerical and Analytical Methods in Geomechanics, 48 (2024) 1949-1978. https://doi.org/10.1002/nag.3714

[8]. H. The, T. Tien and H. Ngoc, Deep Learning-Based Missing Data Reconstruction in SHM Using Gated Dilated Convolution and GRU, International Journal for Numerical Methods in Engineering, 127 (2026), e70257. https://doi.org/10.1002/nme.70257

[9]. M. Görtz, C. Brandl, A. Nitschke, A. Riediger, D. Stromer, M. Byczkowski, V. Heuveline and a. M. Weidemüller, Digital twins for personalized treatment in uro-oncology in the era of artificial intelligence, Nature Reviews Urology, 23 (2026) 29-39. https://doi.org/10.1038/s41585-025-01096-6

[10]. E. M. Dhamani N, Introduction to generative AI, I. Simon and Schuster, 2026.

[11]. H. Minh, T. Sang-To, S. Khatir, M. Wahab, A. Gandomi and T. Cuong-Le, Augmented deep neural network architecture for assessing damage severity in 3D concrete buildings under temperature fluctuations based on K-means optimization, Structures, 57 (2023) 105278. https://doi.org/10.1016/j.istruc.2023.105278

[12]. N.H. Xuan, T.V. Manh, S.N. Nam, L.N. Ngoc, Vibration-based damage detection in cable-stayed bridges using a novel 1D-ConvNeXt-LSTM network, Transport and Communications Science Journal, 77 (2026) 485-499. https://doi.org/10.47869/tcsj.77.4.11

[13]. Q. Le Kha, T.K. Thien, T.N. Thoi, T.N.. Trang, NV. Ho, Reliability-based multi-objective optimization of laminated plates using GDE3 and isogeometric analysis, Transport and Communications Science Journal, 77 (2026) 357-370. https://doi.org/10.47869/tcsj.77.4.2

[14]. H. Hasani and F. Freddi, Condition-aware AI framework for automated structural health monitoring, Automation in Construction, 183 (2026) 106748. https://doi.org/10.1016/j.autcon.2025.106748

[15]. G. Gomes and V. Takano, Strain-based identification of multiple damages in plate-like structures using artificial intelligence and metaheuristic optimization, Machine Learning for Computational Science and Engineering, 2 (2026) 5. https://doi.org/10.1007/s44379-025-00052-w

[16]. A. Ferreira, MATLAB Codes for Finite Element Analysis, Springer, 2008.

[17]. T. Szandała, Review and Comparison of Commonly Used Activation, Bio-inspired neurocomputing, (2020) 203-224. https://doi.org/10.1007/978-981-15-5495-7_11